Blazed transmission grating technology development for the Arcus x-ray spectrometer explorer

Ralf K. Heilmann,[1] Alexander R. Bruccoleri,[2] Jungki Song,[1] Casey deRoo,[3] Peter Cheimets,[3] Edward Hertz,[3] Randall K. Smith,[3] Vadim Burwitz,[4] Gisela Hartner,[4] Marlis-Madeleine La Caria,[4] Carlo Pelliciari,[4] Hans M. Günther,[5] Sarah N. T. Heine,[5] Beverly LaMarr,[5] Herman L. Marshall,[5] Norbert S. Schulz,[5] Eric M. Gullikson,[6] and Mark L. Schattenburg,[1]

[1]Space Nanotechnology Laboratory, MIT Kavli Institute for Astrophysics and Space Research, Massachusetts Institute of Technology, Cambridge, Massachusetts 02139, USA
[2]Izentis LLC, PO Box 397002, Cambridge, MA 02139, USA
[3]Center for Astrophysics, Harvard-Smithsonian Astrophysical Observatory, Cambridge, MA 02138, USA
[4]Max-Planck-Institut für Extraterrestrische Physik, 85748 Garching, Germany
[5]MIT Kavli Institute for Astrophysics and Space Research, Massachusetts Institute of Technology, Cambridge, Massachusetts 02139, USA
[6]Center for X-ray Optics, Lawrence Berkeley National Laboratory, Berkeley, CA 94720, USA

ABSTRACT

Arcus is a high-resolution soft x-ray spectroscopy mid-size Explorer mission selected for a NASA Phase A concept study. It is designed to explore structure formation through measurements of hot baryon distributions, feedback from black holes, and the formation and evolution of stars, disks, and exoplanet atmospheres. The design provides unprecedented sensitivity in the 1.2-5 nm wavelength band with effective area up to $350\,\text{cm}^2$ and spectral resolving power $R > 2500$. The Arcus technology is based on a highly modular design that features 12 m-focal length silicon pore optics (SPO) developed for the European Athena mission, and critical-angle transmission (CAT) x-ray diffraction gratings and x-ray CCDs developed at MIT.

CAT gratings are blazed transmission gratings that have been under technology development for over ten years. We describe technology demonstrations of increasing complexity, including mounting of gratings to frames, alignment, environmental testing, integration into arrays, and performance under x-ray illumination with SPOs, using methods proposed for the manufacture of the Arcus spectrometers. CAT gratings have demonstrated efficiency $> 30\%$. Measurements of the 14th order Mg-$K_{\alpha_{1,2}}$ doublet from a co-aligned array of four CAT gratings illuminated by two co-aligned SPOs matches ray trace predictions and exceeds Arcus resolving power requirements.

More than 700 CAT gratings will be produced using high-volume semiconductor industry tools and special techniques developed at MIT.

Keywords: Arcus, critical-angle transmission grating, x-ray spectroscopy, blazed transmission grating, soft x-ray, grating spectrometer, high resolving power

1. INTRODUCTION

Throughout our universe ubiquitous plasmas emit and absorb at characteristic wavelengths and line intensity ratios that allow us to diagnose and map the physical conditions across a vast range of length scales and densities from the Cosmic Web to the atmospheres of stars. Many of these wavelengths lie in the soft x-ray band between ~ 1 and 5 nm wavelength (or ~ 0.25 and 1.25 keV in photon energy), where high resolving power $R = \lambda/\Delta\lambda$ is best achieved using grating spectrographs. The x-ray grating spectrographs currently in space

- the Reflection Grating Spectrometer (RGS) on XMM-Newton[1] and the High-(HETGS)[2] and Low-(LETGS)[3] Energy Transmission Grating Spectrometers on board Chandra were launched in 1999 with technology from a generation ago. They perform insufficiently to address many contemporary high-priority questions that are best investigated using large effective area, high resolving power soft x-ray spectroscopy.

Arcus[4–6] is a soft x-ray spectroscopy mission that promises up to an order-of-magnitude improvement in relevant figures of merit, leveraging technology developments over the last 2-3 decades. It has been selected for a competed NASA mid-size Explorer (MIDEX) Phase A study, with a decision near the end of 2018.

The enabling technologies for Arcus are Silicon Pore Optics (SPOs - stacks of focusing precision grazing-incidence silicon mirrors developed for the European Athena mission),[7,8] Critical-Angle Transmission (CAT) gratings (lightweight, alignment insensitive blazed transmission gratings developed at MIT and fabricated from silicon-on-insulator (SOI) wafers),[9–15] and state-of-the-art x-ray CCDs (MIT/Lincoln Lab CCID-94 backside illuminated (BI) devices).[6] Combining sub-aperturing with SPOs, Arcus has five times better line response function (LRF) than XMM-Newton. CAT gratings designed for Arcus diffract from 200 nm-period "nanomirror" structures blazed into orders 3-10, providing superior resolving power compared to the HETGS gratings of the same period which are mostly utilized in ± first order. Their diffraction efficiency is on the order of 30% with room for improvement, which significantly exceeds HETGS and LETGS performance.

This paper concentrates on CAT grating technology development for Arcus. CAT gratings feature free-standing, ultra-high aspect ratio grating bars etched out of the device layer of a SOI wafer. Tilting the grating, such that x rays are incident onto the smooth grating bar sidewalls at a graze angle below the critical angle for total external reflection, results in highly efficient diffraction into orders that are near the angle of specular reflection from the sidewalls, which is also known as blazing. The principle has been demonstrated and described in the literature many times over the last decade.[16–22] Over the years diffraction efficiency and grating size have been consistently improved, with 32×32 mm^2 gratings routinely providing on the order of 30% diffraction efficiency. CAT gratings have been demonstrated to be precise enough and compatible with spectrometer designs for $R > 10,000$ at Al-K$_\alpha$ wavelength.[21] No evidence for degraded performance has been found after environmental testing of gratings.[22]

Our recent focus has been on the integration and alignment of arrays of CAT gratings. The goal has been to systematically develop alignment techniques and the underlying metrology to go from relatively simple bread-board demonstrations involving few elements (one SPO and one grating) to increasingly flight-like hardware with all relevant degrees of complexity. Previously we reported on the alignment of two gratings and one SPO. This paper is organized as follows: After a brief overview of the Arcus optical design we describe the successful co-alignment of four gratings and two SPOs and outline our near-term plans for more flight-like demonstrations. Next we discuss efforts regarding MIT in-house x-ray diffraction efficiency testing and the scaling up of grating fabrication, before we finally summarize.

2. ARCUS OPTICAL DESIGN

Arcus consists of four optical channels (OC) with parallel optical axes (see Fig. 1). Each optical channel consists of an optics petal that holds 34 co-aligned silicon pore optics mirror modules (MM) with 12 m focal length, immediately followed by a grating petal with one grating window per MM. Each grating window holds 4-6 (depending on the MM size) co-aligned CAT gratings. The gratings in a petal are all aligned to the surface of a tilted Rowland torus and disperse along the same axis. Each OC generates its own spectrum, which is spread over two x-ray CCD readout arrays. One array receives the non-dispersed zero order (image) transmitted through the gratings, as well as the mostly weak low diffraction orders, while the other array records the more intense higher orders around the blaze angle of the gratings (see Fig. 2). The four optical axes are offset in the cross-dispersion (y) direction by 5 mm from each other, which relaxes relative alignment constraints between the OCs. This compact and modular double tilted-Rowland-torus design keeps the number of x-ray CCDs as low as possible and maximizes resolving power from the limited mirror effective area that can be afforded within an Explorer budget.[23,24] Each optics petal is effectively a sub-aperture of an Athena-like, circularly symmetric Wolter-I mirror assembly. The sub-aperture produces an anisotropic point spread function.[25] By orienting the grating dispersion axes along the narrow dimension of the sub-apertured PSF, the design utilizes the narrowest line response function possible for maximum spectral resolving power.
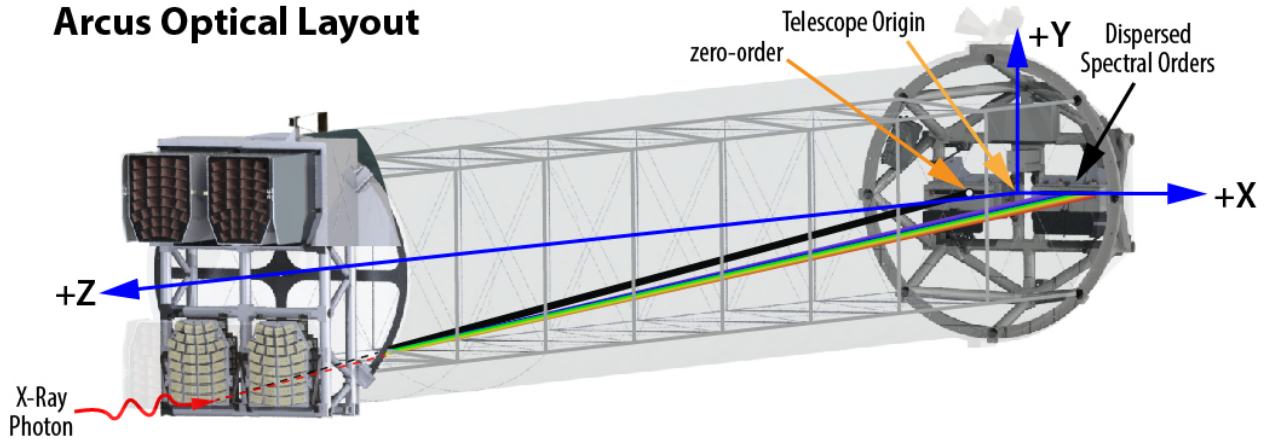
Figure 1. Arcus Optical Layout. X rays enter from the left through thermal pre-collimators, are focused by SPO mirror modules, and dispersed in transmission by CAT gratings. As an example, most x rays entering through the lower left SPO module will either be transmitted to the zeroth order image on the left CCD array or blazed into diffraction orders that are recorded on the right CCD array.
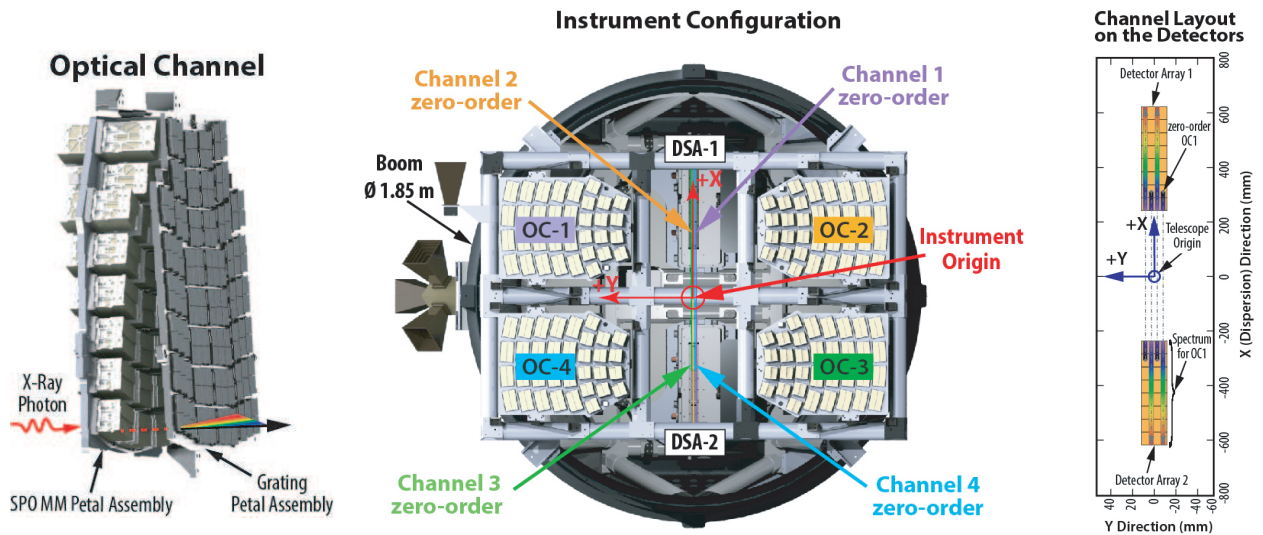

Figure 2. **Left:** Close-up view of an optical channel (OC), consisting of a petal with 34 co-aligned SPO MMs and a co-aligned petal with 34 grating windows, holding a total of 176 gratings. **Middle:** View from the source towards the cameras along the direction of the optical axes for the four OCs. **Right:** Enlarged view of the layout of the four spectra on the detectors (note different scales for x and y).
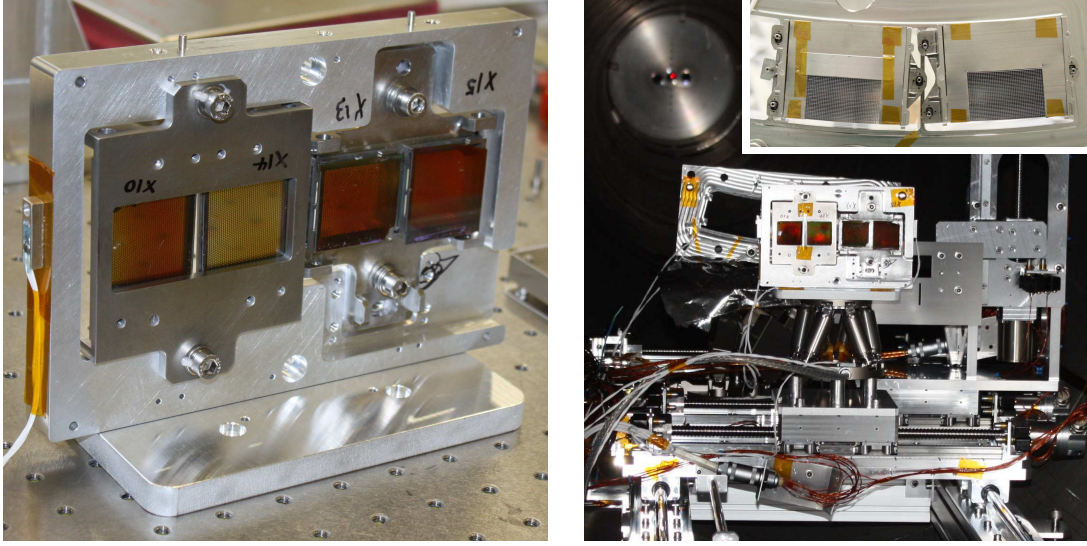
Figure 3. **Left:** Grating petal holding four co-aligned CAT gratings. **Right:** GWAT hardware after installation in the PANTER vacuum tube. The red alignment laser coming from the source (upper left corner) is transmitted through one of the SPOs (not visible, view blocked by grating petal) and transmitted through the second grating from the left. The grating hexapod and two mask stages can also be seen. **Inset:** The two co-aligned SPO XOUs used to illuminate the four gratings simultaneously.

3. GRATING WINDOW ALIGNMENT TEST (GWAT)

Previously we demonstrated roll alignment between two 32×32 mm^2 CAT gratings that were simultaneously illuminated by a single SPO X-ray Optical Unit (XOU), which consists of a stack of primary SPO mirrors aligned to a stack of secondary mirrors.[22] Alignment was first performed in air using a scanning laser reflection tool (SLRT),[26] and then tested with x-rays at the PANTER x-ray facility.[22, 27] The difference in roll angle was found to be $\sim 3.5 \pm 1.2$ arcmin, which is within the conservative five arcmin allocation for Arcus. The Grating Window Alignment Test (GWAT) was designed to gain experience with a higher level of complexity. It features two grating windows, holding two large CAT gratings each (see Fig. 3). To illuminate a significant fraction of each of the four gratings at once, at least two co-aligned SPO XOUs are needed. In this work the bottom XOUs of mirror modules MM-0025 and MM-0027 were used (XOU-0041B and XOU-0048), both with a 737 mm nominal outer radius of curvature. The alignment of the two XOUs (separated by 7.5 degrees center to center in azimuth) to a common focus was performed by Media Lario and is described in detail elsewhere.[28] The resulting PSF clearly shows the anisotropic PSF from the two individual XOUs rotated by 7.5 degrees relative to each other (see left side of Fig. 4).

For the first grating window we re-used the gratings (X10 and X14) and alignment testbed from the previous test. The second window used a modified design for roll angle adjustment and two new gratings (X13 and X15). We often called the windows pseudo-windows, since they are too large for Arcus and block too much area, but for brevity we simply refer to them as windows here. First the gratings within each window were aligned to each other using the same procedure employed previously: The window is scanned under a UV laser beam along a straight line, and the directions of the backdiffracted beam from each grating are compared.[26] The gratings are then adjusted in roll until the directions of the diffracted beams agree to within the required precision. After the gratings in each window are aligned the windows are mounted to a flat grating petal plate with screws. The plate is then scanned under the laser beam, and the roll between the windows is adjusted. Details of the process are described elsewhere.[29] No active effort was made to align the gratings in pitch or yaw; they were simply epoxy-bonded to Ti frames, which in turn were held against the windows with screws. Finally, grating frames and windows were spot-bonded with epoxy to windows and the petal plate, respectively, in an attempt to prevent drift or slippage. Another set of SLRT measurements was done after the epoxy had cured. No change in alignment was found after curing.

The grating petal was taken to PANTER, where it was mounted in the 12 m long, 3.5 m diameter vacuum chamber to a hexapod. It was initially aligned in pitch and yaw to the upstream SPO XOU pair (mounted on a separate hexapod) by eye in air using the back reflection of an alignment laser beam originating from the location of the electron bombardment x-ray source at the far end of the 120 m long vacuum tube connected to the chamber. The distance between gratings and the XOU nodes along the optical axis was measured to be ~ 591 mm. The distance from the gratings to the focus of the XOUs was later determined to be ~ 12736 mm. Due to the finite distance of the source best focus is found at a distance > 12 m from the XOU nodes, and the complete SPO and CAT grating assembly had to be pushed into the vacuum tube to place the focus inside the chamber and within the 500 mm z-travel range of the x-ray camera. A Princeton Instruments x-ray integrating CCD camera (1300×1340 20 μm pixels) was mounted to an xyz linear translation stage stack near the downstream end of the chamber.

After pumpdown, fine centering of the gratings with respect to the XOUs was performed in the plane perpendicular to the optical axis using x rays, and the precise locations of various masks were established. Best focus of the co-aligned XOUs in the dispersion direction was found to be 2.1 arcsec (FWHM, no gratings in the beam). Grating yaw scans in zeroth order show a central maximum which determines the hexapod yaw angle at which the average angle of incidence onto the grating bars is parallel to the grating bar side walls. This angle is different for each grating since the gratings are mounted to a flat plate but sit in a converging beam. For an Arcus grating petal the yaw scan would peak at the same petal yaw angle for all gratings on the petal due to its Rowland torus design.

A zeroth order yaw scan was also performed with all four gratings illuminated at once. From then on the yaw value at the central peak of this scan was used as the "yaw = 0" reference. Using Mg-K$_\alpha$ radiation, the grating petal was then rotated by half the angle of a given diffraction order in order to achieve higher flux in that order (i.e. blazing). We measured the diffraction peaks in 8$^{\text{th}}$ and 10$^{\text{th}}$ order from each grating separately using a movable mask. Roll misalignment between gratings manifests itself through rotation of the dispersion axis around the zeroth order. For small roll angles this primarily moves the diffraction peak in the cross-dispersion direction.

To measure the roll of each grating within the two windows tested as part of the GWAT, the CCD was first translated to the location of the 8$^{\text{th}}$ order Mg K$_\alpha$ centroid for the entire GWAT grating window (i.e. with all gratings illuminated). Leaving the CCD in this fixed location, a given grating was then sub-apertured using a movable mask positioned between the SPO XOUs and the grating windows, thus selecting only the contribution of the given grating to the total diffracted LSF. X-ray data with this single grating sub-aperture was then accumulated, and the centroid of the single grating LSF calculated.

A relative roll misalignment between two gratings can be computed through the approximate relation $\theta = \arcsin(\Delta y/D)$, where θ is the roll misalignment between the two gratings, Δy the offset of the centroids of the two gratings in the cross-dispersion direction, and D the distance dispersed (≈ 504 mm in 8$^{\text{th}}$ order for the GWAT spectrometer). Using a single grating (X10) as a reference, the roll misalignment of each grating in the two grating windows was computed. The average misalignment of the three gratings to the reference grating was found to be < 1 arcmin (1σ), below the alignment allocation for the gratings within an Arcus grating window (5 arcmin). A more detailed comparison between the x-ray measurements and the roll misalignments as measured using the SLRT can be found elsewhere in these proceedings.[29]

Subsequently we investigated 14$^{\text{th}}$ order Mg-K$_\alpha$ at a diffraction angle of almost 4 degrees from zeroth order. Modeling of the resolving power of our system is easier with dispersion data from higher orders, since there the mirror LSF comprises a smaller fraction of the width of any spectral features. The tradeoff is much reduced diffraction efficiency above the critical angle for total external reflection, which for Si at this wavelength is ~ 1.35 degrees. The grating petal yaw angle was set to ~ 1.98 degrees, or half the diffraction angle for this order. This is slightly larger than the design angle of 1.8 deg. for Arcus. Due to the reduced efficiency above the critical angle for this wavelength and long integration times, only data with all four gratings illuminated at once was taken.

The measured 14$^{\text{th}}$ order Mg-K$_\alpha$ data was fit to determine what, if any, contribution the grating assembly made to the diffracted LSF. This fitting serves to place a lower bound on the resolving power of the GWAT
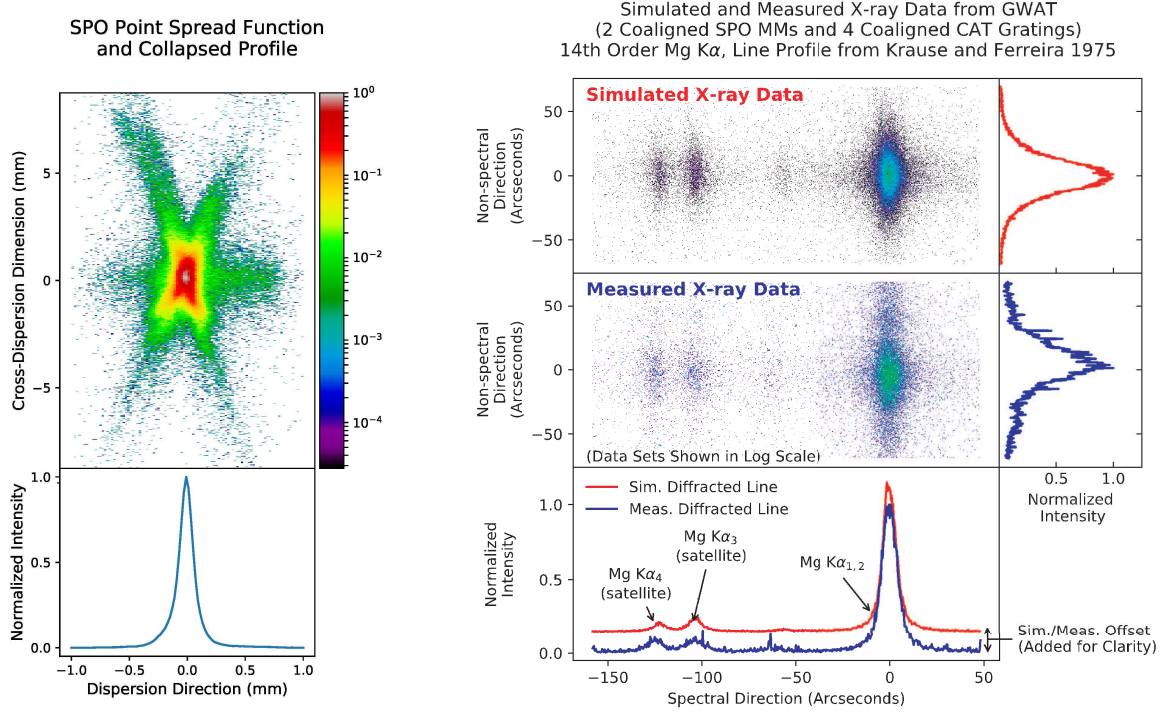
Figure 4. **Left,top:** In-focus anisotropic point-spread function of the two co-aligned SPO XOUs, rotated by 7.5 degrees relative to each other. Logarithmic intensity scale. The PSF is much narrower in the dispersion direction than in the cross-dispersion direction. **Left, bottom:** Projection of the PSF onto the dispersion axis, producing the line response function (LRF). **Right:** Simulated (via ray tracing) and measured data for Mg-K 14th order diffraction peaks.

spectrometer system. To perform this analysis, a well-sampled measurement of the point spread function (PSF) of the SPO XOUs was summed in the cross-dispersion direction. This yields an intensity profile as a function of position along the dispersion axis. Assuming a flawless grating assembly, this summed SPO profile would be the LSF of an infinitely narrow x-ray line. Next, we constructed a model of the Mg-K$_\alpha$ emission complex. This model is based on parameters measured by Krause and Ferreira,[30] assumes line widths of 0.36 eV for the Mg K$_{\alpha_{1,2}}$ doublet, and assumes that the Mg K$_{\alpha_{1,2}}$ peaks are separated by 0.3 eV (Mg K$_{\alpha_1}$ at 1253.7 eV, K$_{\alpha_2}$ at 1253.4 eV). We adopted these parameters as they are among the narrowest reported in the literature, and hence offer a conservative estimate of the resolving power of the CAT gratings tested with the GWAT system. Finally, a potential grating contribution was modeled as a Gaussian for which the FWHM is equal to the central wavelength of the line divided by the maximum resolution of the grating assembly R_{grat}. These components - the SPO PSF, the natural line profile, and the grating contribution - are convolved to yield a model of the diffracted LSF, which is fit to the measured data using the free parameter R_{grat}. Using this method, we find a best fit grating contribution of $R_{grat} \approx 3500$. Furthermore, we compute that the 3σ lower bound on the grating contribution, inferred from the confidence in the fit parameters, exceeds the Arcus resolution requirements. Thus, this measurement and subsequent analysis lend confidence that the current generation of CAT gratings and alignment techniques are capable of meeting the resolution requirements of Arcus.

Finally, to assess our ability to model the performance of the GWAT optical system, we constructed a detailed ray-trace model employing the as-measured optical parameters and performance of the SPO XOUs, the sizes and positions of the gratings within the windows/assembly, the roll misalignments between the gratings as measured with the SLRT, and the positions and orientations of the SPO XOUs and gratings relative to each other. The comparison between the simulated and measured datasets can be seen in Figure 4. The good agreement validates that the ray-tracing models used to simulate the performance of Arcus are quite consistent
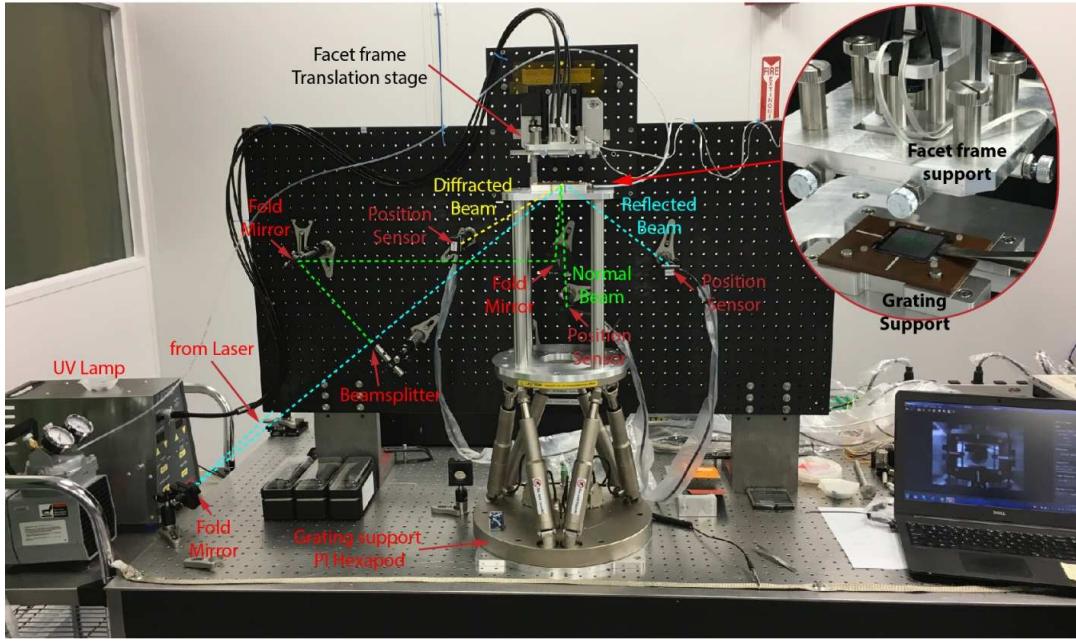
Figure 5. Front view of the Grating Facet Alignment Station (GFAS). The hexapod holds the grating support, and SLRT metrology is performed on the downward-facing grating. The facet frame is lowered from above. The inset shows a close-up of the grating and facet frame supports.

with physical measurements.

4. ALIGNMENT AND BONDING WITH THE GRATING FACET ASSEMBLY STATION

The grating pseudo windows used for the GWAT demonstration served as simple grating holders for manual precision roll alignment using metrology feedback from the SLRT. Obviously they take up too much space, as do the frames that the gratings were bonded to. For Arcus a different design will be used. Arcus Si CAT grating membranes are 26×27 mm^2 in size, with a 2 mm edge all around. Currently one edge has an additional tab near one corner for ease of handling. New flexured Ti frames have been designed and manufactured with a footprint that is fully covered by the grating membrane edge.

For Arcus our goal is to accommodate grating membrane degrees of freedom in the process of bonding a membrane to its frame. Once membrane and frame are bonded and form a so-called grating facet, the sides of the frame will be used as mechanical reference in the alignment and assembly of facets within a grating window. Similarly, window surfaces will be used as mechanical references in the placement of windows on a grating petal.

Translational degrees of freedom for the grating membrane centers are relaxed, with the tightest being 200 μm along the optical (z) axis. Rotational degrees of freedom are controlled under metrology feedback during bonding. The process is the following:

We combine the SLRT with a precision hexapod and a high repeatability vertical translation stage to create a Grating Facet Assembly Station (GFAS). It provides a means for producing grating facets that are interchangeable with any of 700+ grating facets used in Arcus. The GFAS precisely aligns the mounting interface of every facet frame to the grating bars of its companion CAT grating prior to bonding the grating to the facet frame.

First, we select a grating to be the alignment master reference grating. All subsequent gratings will be aligned to the SLRT scans produced during the initial measurements of this grating. The master grating will be periodically rescanned throughout the assembly of the 700+ facets. A grating frame is loaded into the frame support that resides on the vertical translation stage. The stage is configured to transfer the facet frame
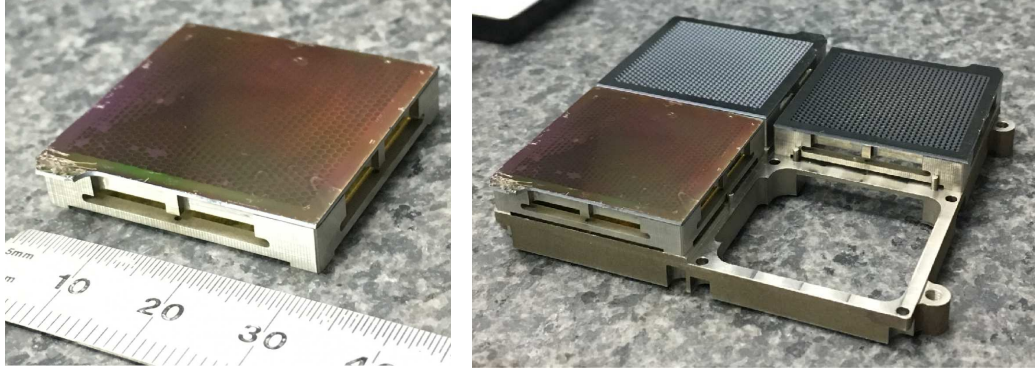
Figure 6. **Left:** Arcus flight-like CAT grating facet, consisting of the Si grating membrane bonded to an athermal Ti flexure frame. **Right:** Flight-like grating window, populated with one grating facet and two grating facet dummies.

from above to the same bond position in space in a highly repeatable manner, with the side to be bonded facing downward. Next, a CAT grating membrane is placed with three of its 2 mm edges onto three horizontal precision machined surfaces on the grating support plate with two edges resting (horizontally "nudged") against three vertical pins forming a kinematic support for the grating. The device layer side of the grating membrane is facing down. Light vacuum is applied through the center of the three support surfaces to hold the grating in place throughout the alignment process. We have verified that the light vacuum does not introduce distortion to the grating membrane. We lower the facet frame into place (nominally 0.20 mm from the grating) and center the grating with the hexapod under the facet frame using a camera located in the facet frame translation assembly. The camera is able to easily discriminate between the inner wall of the facet frame and the edge of the grating membrane at the 50-75 μm level.

After centering, the frame is raised back up out of the way and a small amount of UV curable epoxy is dispensed at the four bond locations on the outer edge of the grating (on the upwards-facing handle layer side with the hexagonal support mesh). We then use the SLRT and the hexapod to scan the grating along its nominal dispersion direction to establish its initial roll orientation. The required roll offset needed to align the grating to the reference scan is commanded to the hexapod and we rescan. This step can be repeated if necessary. Finally, because the grating bars of every CAT grating are not perfectly orthogonal to the membrane surface, we must compensate for the average grating bar tilt angle (measured beforehand with a different tool)[29] by rotating the grating about an axis that passes through the center of the grating membrane surface and is parallel to the grating bars; the hexapod is ideal for this operation. We rotate by the required angle, lower the facet frame into the epoxy, and flash a UV lamp to cure the epoxy. We use a four-pole UV fiber bundle to bond all four grating bonds at once. At this point, the vacuum is turned off, and the grating facet is removed from the GFAS and undergoes a post-UV thermal cure (110°C for 15 minutes) to achieve full bond strength in the epoxy joint. We have verified that the post-UV thermal cure does not distort the grating.

5. FLIGHT-LIKE ALIGNMENT TEST (FLAT)

The flight-like alignment test is similar to the GWAT, but features higher-fidelity, flight-like components and alignment and assembly procedures. Up to four Arcus-sized grating facets will be produced using the alignment and bonding station and following the procedure designed for Arcus flight gratings. The facets will then be mounted to an Arcus-like grating window, using machined window features and frame side walls as mechanical alignment reference structures. The window geometry will place the grating facets onto a Rowland torus surface. After mounting, the relative alignment between the facets in roll, pitch, and yaw will be verified using the SLRT. For x-ray testing another new component will be added. Previous tests have used SPO XOUs built from mandrels of the same radius. For the FLAT we will use a full SPO MM, which requires two co-aligned XOUs with different outermost radii. The production of such MMs is currently making good progress in Europe. Environmental testing of the grating window, bracketed by SLRT and x-ray metrology, is planned as well. The
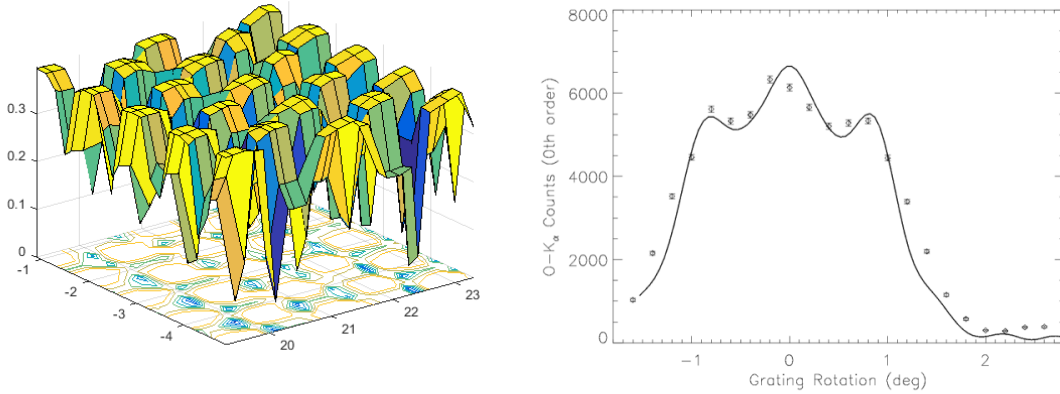
Figure 7. **Left:** Absolute diffraction efficiency (sum of orders 3-8) as a function of position on grating X14 at wavelength $\lambda = 2.38$ nm. This measurement was taken at beamline 6.3.2 of the Advanced Light Source in Berkeley, CA. The average absolute efficiency over the shown 4×4 mm^2 area is 31.6%, *including* blockage from the L1 and L2 support structures. **Right:** Measured x-ray counts in zeroth order O-K line vs. yaw angle for CAT grating X16. Data points measured in the MIT polarimetry beamline are plotted as circles. Synchrotron data for a similar CAT grating are overlayed as a solid line.

window structure has already been fabricated, and the first Arcus-like grating facet has been produced using the above procedures (see Fig. 6).

6. MIT POLARIMETRY BEAMLINE

CAT grating x-ray diffraction efficiency is an essential performance parameter for Arcus. It has been measured for many gratings over the years at beamline 6.3.2 of the Advanced Light Source at Lawrence Berkeley National Laboratory in Berkeley, CA (see the left side of Fig. 7). While this synchrotron is a powerful x-ray source and the beamline is conveniently set up for measurements across the soft x-ray and EUV band, there are advantages to having a dedicated in-house x-ray grating characterization facility: lack of time-consuming travel and facility availability around the clock with the possibility of highly automated measurements.

The MIT polarimetry beamline has been re-configured and upgraded from its original purpose as a 20-m long calibration facility for the Chandra HETG gratings.[31,32] The beamline has three chambers (source, grating and detector). Source and gratings are ~ 10 m apart from each other. The X-ray source is a Manson source with several interchangeable anodes to produce various line energies. The grating chamber allows horizontal control of the apertures and slits, and horizontal, vertical and rotational control of gratings. The detector chamber contains a Princeton Instruments CCD detector, which is mounted on a X-Y stage so that the detector can be moved to intercept different regions of the incoming dispersed beam. Since CAT gratings disperse further than HETG gratings, the distance between the grating chamber and the detector chamber was shortened to ~ 2 m.

We now routinely characterize CAT gratings in orders 0-7 at the Arcus-relevant O-K wavelengths, using a sapphire target. Measured absolute efficiencies are consistent with results from synchrotron tests (see the right side of Fig. 7). The level of automation for collecting data has been increased. In the near future, collection of a comprehensive set of measurements across several CAT gratings will be fully automatic.

7. FABRICATION

All CAT gratings produced to date, and utilized in the tests reported here, were fabricated using laboratory nanofabrication tools available on the MIT campus. The fabrication procedure, as developed and reported over the last decade, involves a complex set of double-sided lithographic processing steps using custom-fabricated silicon-on-insulator substrates which are becoming increasingly popular in the semiconductor industry.[15] This fabrication procedure, as currently constituted, comprises over 125 steps, and is designed to use "tweezer and beaker" processing tools available on the MIT campus, which are generally limited to 100 mm wafer diameters.

It has become clear that this process and tool set are inadequate to produce the more than 700 large, high-quality gratings required for Arcus on the time scale available to an Explorer mission.

We have been fortunate to recruit the MIT Lincoln Laboratory (MIT-LL) microfabrication team to this effort. This is the same group that developed advanced CCD chips for Chandra, Suzaku, and TESS. The MIT-LL team has access to the advanced Microfabrication Laboratory foundry for 200 mm-diameter silicon wafers with advanced robot-loaded lithographic patterning and etch tools. We are in the process of transferring the front end of our process (front and back side silicon oxide patterning) to the automated tools of the LL foundry. During Phase B of the proposed Arcus effort we will transfer the back end of the process to new tools situated in MIT campus clean room facilities. This proposed demarcation of the process between campus and LL facilities leverages the considerable strengths of the LL foundry, which is optimized for high fidelity thin-film patterning, while performing the more exotic deep-etch processes pioneered over the last decade on the MIT campus.

8. SUMMARY

Arcus is a high-resolution soft x-ray spectroscopy Explorer mission with an exciting and timely science case. X-ray optics, grating, and CCD technology have made much progress in the decades since the last x-ray grating spectrometers were designed, built, and launched into space on board expensive Observatory-class missions. It is not surprising that a much more powerful instrument can be built today within a much smaller Explorer budget. CAT gratings are an enabling technology for Arcus and have been fabricated, aligned, and tested in increasingly flight-like configurations. Our tests, performed with international collaboration and coordination, have met Arcus alignment and performance requirements on schedule. We continue to develop metrology for grating characterization and alignment and technology for integration into large arrays. At the same time we are preparing for increased automation of the grating fabrication process. Should Arcus be selected to proceed into Phase B we are well prepared to build a successful mission.

ACKNOWLEDGMENTS

REFERENCES

[1] den Herder, J. W. *et al.*, "The reflection grating spectrometer on board XMM-Newton," *Astr. & Astroph.* **365**, L7-L17 (2001).

[2] Canizares, C. R. *et al.*, "The Chandra high-energy transmission grating: Design, fabrication, ground calibration, and 5 years in flight," *PASP* **117**, 1144-1171 (2005).

[3] Pease, D., Drake, J. J., Kashyap, V., Marshall, H. L., Raffauf, E. L., Ratzlaff, P. W., Wargelin, B. J., "In-flight effective area calibration of the Chandra low energy transmission grating spectrometer," *Proc. SPIE* **4851**, 157 (2003).

[4] Smith, R. K. *et al.*, "Arcus: the x-ray grating spectrometer explorer," *Proc. SPIE* **9905**, 99054M (2016).

[5] Brenneman, L. W., *et al.*, "The evolution of structure and feedback with Arcus," *Proc. SPIE* **9905**, 99054P (2016).

[6] Smith, R. K. *et al.*, "Arcus: Exploring the formation and evolution of clusters, galaxies, and stars," *Proc. SPIE* **10397**, paper 27, to be published (2017).

[7] Collon, M. J., Ackermann, M., Günther, R., Chatbi, A., Vacanti, G., Vervest, M., Yanson, A., Beijersbergen, M. W., Bavdaz, M., Wille, E., Haneveld, J., Olde Riekerink, M., Koelewijn, A., van Baren, C., Müller, P., Krumrey, M., Burwitz, V., Sironi, G., and Ghigo, M., "Making the Athena optics using silicon pore optics," *Proc. SPIE* **9144**, 91442G (2014);

[8] Collon, M. J. *et al.*, "Silicon pore optics mirror module production and testing," *Proc. SPIE* **10699**, these proceedings (2018).

[9] Ahn, M., Heilmann, R. K. and Schattenburg, M. L., "Fabrication of ultrahigh aspect ratio freestanding gratings on silicon-on-insulator wafers," *J. Vac. Sci. Technol. B* **25**, 2593-2597 (2007).

[10] Ahn, M., Heilmann, R. K. and Schattenburg, M. L., "Fabrication of 200 nm-period blazed transmission gratings on silicon-on-insulator wafers," *J. Vac. Sci. Technol. B* **26**, 2179-2182 (2008).

[11] Mukherjee, P., Bruccoleri, A., Heilmann, R. K., Schattenburg, M. L., Kaplan, A. F. and Guo, L. J., "Plasma etch fabrication of 60:1 aspect ratio silicon nanogratings on 200 nm pitch," *J. Vac. Sci. Technol. B* **28**, C6P70-5 (2010).

[12] Bruccoleri, A., Mukherjee, P., Heilmann, R. K., Yam, J. and Schattenburg, M. L., "Fabrication of nanoscale, high throughput, high aspect ratio freestanding gratings," *J. Vac. Sci. Technol. B* **30**, 06FF03 (2012).

[13] Bruccoleri, A. R., Guan, D., Vargo, S., DiPiazza, F., Heilmann, R. K. and Schattenburg, M. L., "Nanofabrication advances for high efficiency critical-angle transmission gratings," *Proc. SPIE* **8861**, 886119 (2013).

[14] Bruccoleri, A. R., Guan, D., Mukherjee, P., Heilmann, R. K., Schattenburg, M. L. and Vargo, S., "Potassium hydroxide polishing of nanoscale deep reactive-ion etched ultra-high aspect ratio gratings," *J. Vac. Sci. Technol. B* **31**, 06FF02 (2013).

[15] Bruccoleri, A. R., Heilmann, R. K., and Schattenburg, M. L., "Fabrication Process for 200 nm-Pitch Polished Freestanding Ultra-High Aspect Ratio Gratings," *J. Vac. Sci. Technol. B* **34**, 06KD02 (2016).

[16] Heilmann, R. K., Ahn, M., Gullikson, E. M. and Schattenburg, M. L., "Blazed high-efficiency x-ray diffraction via transmission through arrays of nanometer-scale mirrors," *Opt. Express* **16**, 8658-8669 (2008).

[17] Heilmann, R. K., Ahn, M. and Schattenburg, M. L., "Fabrication and performance of blazed transmission gratings for x-ray astronomy," *Proc. SPIE* **7011**, 701106 (2008).

[18] Heilmann, R. K. *et al.*, "Critical-angle transmission grating spectrometer for high-resolution soft x-ray spectroscopy on the International X-Ray Observatory," *Proc. SPIE* **7732**, 77321J (2010).

[19] Heilmann, R. K., Ahn, M., Bruccoleri, A., Chang, C.-H., Gullikson, E. M., Mukherjee, P. and Schattenburg, M. L., "Diffraction efficiency of 200 nm period critical-angle transmission gratings in the soft x-ray and extreme ultraviolet wavelength bands," *Appl. Opt.* **50**, 1364-1373 (2011).

[20] Heilmann, R. K., Bruccoleri, A. R., and Schattenburg, M. L., "High-efficiency blazed transmission gratings for high-resolution soft x-ray spectroscopy," *Proc. SPIE* **9603**, 960314 (2015).

[21] Heilmann, R. K., Bruccoleri, A. R., Kolodziejczak, J., Gaskin, J. A., ODell, S. L., Bhatia, R., and Schattenburg, M. L., "Critical-Angle X-ray Transmission Grating Spectrometer with Extended Bandpass and Resolving Power > $10,000$," *Proc. SPIE* **9905**, 99051X (2016).

[22] Heilmann, R. K., Bruccoleri, A. R., Song, J., Kolodziejczak, J., Gaskin, J. A., ODell, S. L., Cheimets, P., Hertz, E., Smith, R. K., Burwitz, V., Hartner, G., La Caria, M. M., and Schattenburg, M. L., "Critical-angle transmission grating technology development for high resolving power soft x-ray spectrometers on Arcus and Lynx," *Proc. SPIE* **10399**, 1039914 (2017).

[23] Günther, H. M. *et al.* "Performance of a double tilted-Rowland-spectrometer on Arcus," *Proc. SPIE* **10397**, 103970P (2017).

[24] Günther, H. M. *et al.* "Ray-tracing Arcus in Phase A," *Proc. SPIE* **10699**, these proceedings (2018).

[25] Cash, W., "X-ray optics: a technique for high-resolution imaging," *Appl. Opt.* **26**, 2915 (1987).

[26] Song, J., Heilmann, R. K., Bruccoleri, A. R., Hertz, E., and Schattenburg, M. L., "Scanning laser reflection tool for alignment and period measurement of critical-angle transmission gratings," *Proc. SPIE* **10399**, 1039915 (2017).

[27] Burwitz, V. *et al.*, "In focus measurements of IXO type optics using the new PANTER x-ray test facility extension". *Proc. SPIE* **8861**, 88611J (2013).

[28] Valsecchi, G. *et al.*, "Results of silicon pore optics mirror modules optical integration of the ATHENA telescope," these proceedings (2018).

[29] Song, J., Heilmann, R. K., Bruccoleri, A. R., Hertz, E., and Schattenburg, M. L., "Metrology for quality control and alignment of CAT grating spectrometers," *Proc. SPIE* **10699** (these proceedings, 2018).

[30] Krause, M. O., and Ferreira, J. G., K x-ray emission spectra of Mg and Al," J. Phys. B: Atom. Molec. Phys. **8**, 2007 (1975).

[31] Dewey, D., Humphries, D. N., McLean, G. Y. and Moschella, D. A., "Laboratory calibration of x-ray transmission diffraction gratings," *Proc. SPIE* **2280**, 257 (1994).

[32] Heine, S. N. T., Marshall, H. L., Heilmann, R. K., Schulz, N. S., Beeks, K., Drake, F., Gaines, D., Levey, S., Windt, D. L., and Gullikson, E. M., "Laboratory progress in soft x-ray polarimetry," *Proc. SPIE* **10399**, 1039916 (2017).